The 4-Point Backyard Diurnal Parallax Method Tested on a Challenging Far Away Target: Dwarf Planet 134340 Pluto

Eduardo Manuel Álvarez
Observatorio Los Algarrobos, Salto, Uruguay
Costanera Sur 559, Salto 50.000, URUGUAY
olasu@adinet.com.uy

Robert K. Buchheim
Altimira Observatory
Coto de Caza, CA 92679, USA
Bob@RKBuchheim.org

Abstract

Asteroid distances can be easily determined using an amateur-level telescope and CCD from a single station, not requiring any data other than strictly derived from direct observations. Despite the simplicity of the 4-Point Backyard procedure – which only necessitates observations from two consecutive nights, just obtained at the beginning of each night and at each culmination – we had achieved an excellent accuracy for a set of asteroids out to a distance of 2.6 au.

Now we have pushed the simple backyard diurnal parallax method in order to test its viability on a previously inconceivably distant target – Pluto – placed at more than ten times as far away our previous furthest measured asteroid. Surprisingly, our results were much better than expected. This project demonstrates the suitability of the method despite its evident simplicity, no matter how distant the asteroid target is. However, there are some special considerations with a distant target to ensure that the astrometry is performed with due care.

1. Introduction

Nowadays no one would seriously think of using diurnal parallax for determining an accurate distance to a Solar System object. If its distance hasn't yet been precisely determined, there are other simpler ways to measure it. However, at the amateur (or student) level the observation of diurnal parallax is an attractive project because of two important attributes: (a) it remains one of the few demonstrations of the Earth's daily rotation that can be easily carried on; and (b) it becomes a rewarding learning experience for those who dare to measure it.

On a previous paper (Alvarez and Buchheim, 2012) we had presented a detailed mathematical analysis about the general diurnal parallax effect and how it can be easily measured from a single location in order to determine asteroid distances by using just a small-aperture telescope and a CCD camera. We also supplied evidence of having achieved 5% or better accuracy on a handful of asteroids placed at different distances, from 0.05 astronomical units (au) up to 2.56 au. We concluded our paper stating that in principle our simple self-contained method could be used for finding out the parallax of much more distant Solar System objects, or even nearby stars.

This paper is all about picking up the gauntlet regarding the first challenge: to test the suitability of our backyard diurnal parallax method on a Solar System object placed at far beyond the asteroid belt zone. We chose Pluto to work with – meaning we were going to dive into subarcsecond waters.

Amateur gear is usually not quite appropriate to deal with subarcsecond issues. Usual sources of error at the normal level of a few arcseconds are still comfortably managed by small-sized telescopes and CCDs by means of proper measuring techniques. However, attempting to descend one full order of magnitude in order to perform accurate astrometry at the subarcsecond level poses serious troubles. Atmospheric refraction and dispersion certainly introduce distortion that does affect measurements, as well as optical aberrations and tracking errors – to name just a few.

Richard Berry (2011) reported that by means of differential astrometry he was able to measure relative coordinates of Barnard's Star with an 8-inch telescope to a precision of 1 sigma of 0.01 arcsecond. This feat was accomplished by taking a large number of images (~60) each night, and making all of them quite near the Meridian plane. Unfortunately, neither of these principles could be extrapolated to our austere 4-Point Backyard parallax procedure: all four

sets of required images must be made in relatively narrow time windows (about 10 minutes) and also half of them necessarily must be taken at low sky altitudes (i.e., high air mass).

Given such restrictions, a priori it seemed that attempting the measurement of Pluto's diurnal parallax was going to be a losing battle. Against all the odds, we took the plunge – the idea of measuring parallactic angles becomes some sort of siren call to some of us. Fortunately, we could arrive at safe land – Pluto's parallax was satisfactory measured. Also, the endeavor did happen to be a rewarding learning experience.

2. The Diurnal Parallax Effect

Parallax is a widely-understood and easily demonstrated phenomenon, as is its derived practical benefit – to allow determining the distance to an object without directly measuring it. In theory, once the parallactic shift of the apparent position of a distant object is measured (by observing from the ends of a baseline of known length), then its distance can be readily determined. In practice, taking into account that in most astronomical applications the parallax angle is very small, the only way to take advantage of this technique for distance determination is by means of using a very large baseline.

Placed on the Earth's surface, any observer is actually moving along a perfectly circular track, several thousand kilometers in radius, making one complete circle each 23.93 hours – the sidereal period. At any given time, the observer is seeing the vault of heaven from a slightly different and continuously varying perspective compared to a fictitious observer placed at rest at the center of the Earth. The apparent waving displacement of relatively nearby celestial objects with respect to distant "fixed" stars as observed from any ground site, exclusively due to Earth's daily rotation, is known as the diurnal parallax effect. This effect materializes as a very subtle angular oscillation, varying from a few hundreds of arcseconds for sufficiently close Near Earth Objects, down to barely tenths of arcseconds for the furthest observable Solar System objects. The diurnal parallax effect is immeasurably small for celestial bodies beyond the Solar System.

The diurnal parallax effect has nothing to do with the fact that any given Solar System object is moving with respect to the center of the Earth. Figure 1 exemplifies how these totally independent effects actually appear in the sky. Comparatively, the apparent celestial motion of any Solar System body due to its orbital revolution around the Sun becomes orders of magnitude larger than its corresponding diurnal parallax effect.

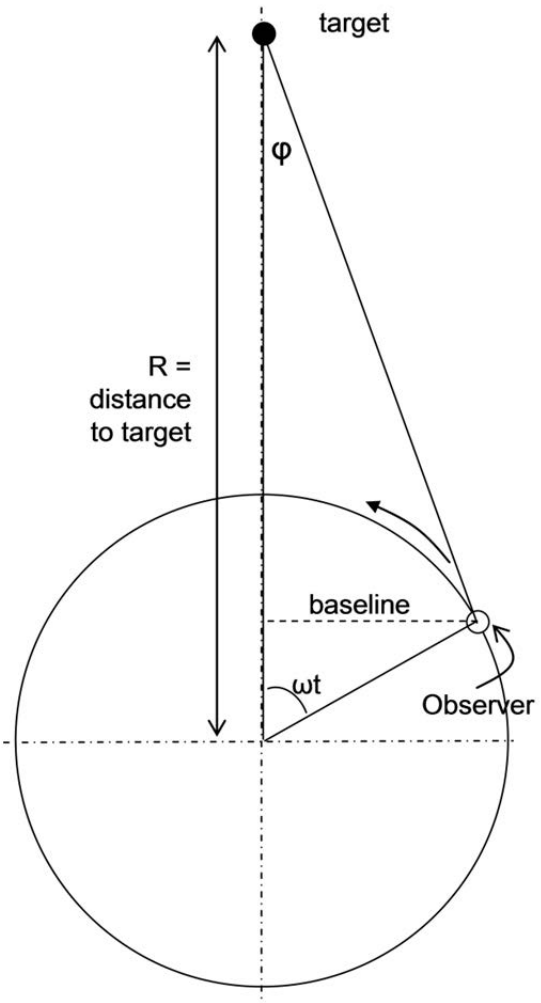

Figure 1. Geometry of the diurnal parallax effect. As the Earth rotates, any observer on its surface sees the target's parallactic angle *φ* constantly varying, from a maximum value occurring when his Meridian is at right angle to the plane containing the Earth's rotation axis and the target (some 6 hours prior or after transit time) to a null value whenever the target happens to be placed on his Meridian (target culmination).

Therefore, not only must the measurement of diurnal parallax deals with minuscule oscillating displacements with respect to "fixed" stars, but at the same time such tiny effects are always encapsulated within much larger "proper motion" displacements across the sky. Consequently, the first move in the diurnal parallax game consists of accurately subtracting the dominant orbital trajectory across the sky from the actually observed apparent celestial motion of the target in question. If carefully and properly done, what remains after this sieving – usually referred to as 'residuals' – is only due to the diurnal parallax effect.

Assuming that for a time period as short as a couple of days the distance from the Earth's center to the target is basically constant – a generally appropriate assumption except for nearby NEO asteroids and the Moon – then the time variability of the parallactic angle can be exclusively attributed to the observer's changing position relative to a fixed direction in the equatorial plane. In other words, with respect to the plane that contains the axis of rotation of the Earth (i.e., in declination) the parallax angle remains basically invariant. This is why the diurnal parallax is also called the east-west parallax. The diurnal parallax effect exactly corresponds to the variable parallactic angle – the angle that at any given moment has the target on its vertex, the observer on one side and the center of the Earth on the other side – projected to the equatorial plane. It's clear that at the moment of the target's culmination (when the target happens to be on the observer's Meridian) the variable diurnal parallax angle becomes null, while achieving its maximum theoretical value some 5.98 hours (¼ of sidereal period) either before or after transit. (It would be at exactly ¼ of the sidereal period if the target were not moving with respect to Earth's center.)

Therefore, by definition, at any given time t the variable diurnal parallax angle φ becomes

$$\varphi(t) = [RA_{topo}(t) - RA_{geo}(t)]\cos\delta(t) \qquad \text{Eq. 1}$$

where RA_{topo} is the object's topocentric (measured from the observer location) right ascension, RA_{geo} is the object's geocentric (measured from the center of the Earth) right ascension, and δ is the object's declination (assumed to be practically the same as measured either from the observer's place or from the center of the Earth).

For observations taken before transit, the parallactic projection of the target on the background star field makes it appear to the observer as displaced towards the east with respect to what would be observed at the same time from Earth's center – that is, before transit: $RA_{topo}(t) > RA_{geo}(t)$. Conversely, the parallactic projection appears displaced towards the west for observations that take place after transit – that is, after transit: $RA_{topo}(t) < RA_{geo}(t)$. Therefore, the variable diurnal parallax angle $\varphi(t)$ as defined by Equation 1 becomes positive for observations taking place before transit, and negative for observations taking place past transit.

As Earth rotates, the term inside the square brackets $[RA_{topo}(t) - RA_{geo}(t)]$ varies as the observer is carried long by Earth's rotation, reaching its maximum whenever the observer and the target happen to be placed at right angles with respect to the Earth's center. Meanwhile, taking into account that the target's declination does vary – gradually – with time but totally independent of Earth rotation, the term cos $\delta(t)$ changes only slightly during a short time period of a few days. Therefore, the variable diurnal parallax angle basically varies on a daily basis as a sinusoidal function, at any time having a value equal to $[RA_{topo}(t) - RA_{geo}(t)]$ times the almost constant cosine of the target's declination.

From Figure 1, at any given time t the length of the projected observational baseline B becomes:

$$B(t) = R_E \cos\lambda \sin(\omega t) \qquad \text{Eq. 2}$$

where R_E is the radius of the Earth, λ is the latitude of the observer, ω is the angular sidereal rotation rate of the Earth, and the beginning of time ($t = 0$) has been conveniently chosen to make it coincide with the moment of the target culmination. This baseline varies sinusoidally as Earth rotates, achieving its maximum value B_{max} each time ωt equals 90º – that is, when the observer and the target also happen to be placed at right angle with respect to the Earth's center.

Once the variable diurnal parallax angle and corresponding projected baseline are known, the distance R to the target can be readily obtained by making use of the small-angle approximation:

$$R = \frac{B(t)}{\varphi(t)} \qquad \text{Eq. 3}$$

where B and R have to be expressed in the same units and the angle φ is in radians.

In practice, whenever the parallactic angle of a target is mentioned without any further specification, it is usually referred to the maximum value that Equation 1 can achieve. In order to avoid confusion between the variable diurnal parallax angle $\varphi(t)$ and the maximum value such parameter could achieve, we will explicitly refer to the later as the Diurnal Parallax Maximum Angle (φ_{max}).

3. The Simplified Method

From Equation 1 the variable parallactic angle can be readily obtained for any given time. The quality of the Diurnal Parallax Maximum Angle output comes hand in hand with the accuracy of the two required time-dependent parameters: (a) the target's topocentric coordinates data, and (b) the target's geocentric right ascension data.

The target's topocentric coordinates (both right ascension and declination) can be actually measured

by the observer at any time. On the contrary, the required target's geocentric right ascension simply cannot – except at just the precise moments when both topocentric and geocentric target's right ascension happen to coincide. This occurs when the target, the observer and the Earth's center all happen to be in the same plane – the Meridian.

At the fleeting moment when the target crosses the Meridian – in other words, at the exact time *T0* when the target culminates – it becomes true that $RA_{topo}(T0) = RA_{geo}(T0)$. Therefore, the variable target's geocentric right ascension can be inferred from actual measurements obtained once per night. From two consecutive culminations, the target's geocentric right ascension can be estimated by a linear motion; from three culminations, by a quadratic motion; from four culminations, by a third order motion; and so on.

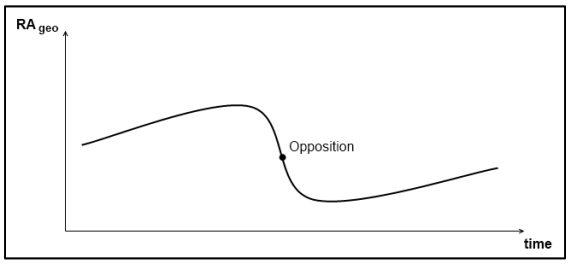

Figure 2. The apparent motion in right ascension of a minor planet. Most of the time it displaces towards higher RA values (direct motion) but once a year, as it approaches the closest distance to Earth, it appears moving backwards to lower RA values for a while (retrograde motion).

Figure 2 shows the typical yearlong geocentric right ascension displacement for an asteroid. RA_{geo} steadily increases (direct motion) up to a moment when it becomes reversed for a while (retrograde motion), until later on resuming its "normal" direct motion. Opposition occurs near the middle of the retrograde loop. Note that around opposition the asteroid happens to be at minimum distance from Earth, but also the RA_{geo} rate achieves its highest value and the RA motion is quite linear (second order derivative becomes null).

Figure 3 shows the actual negative concavity of RA_{geo} motion before opposition, and the corresponding linear approximation derived from just two observed consecutive transits (on night 1 and night 2). Similarly, Figure 4 shows the actual positive concavity of RA_{geo} motion after opposition, and the corresponding linear approximation derived from just two observed consecutive transits.

During first half of the retrograde loop, when the asteroid has not yet reached opposition, at any given time (Obs_1) prior to the first transit ($T0_1$) the RA_{geo} value estimated by linear approximation (E_1) is always larger than the actual "true" value (A_1). On the contrary, at any given time (Obs_2) also prior to the second transit ($T0_2$), the RA_{geo} value estimated by linear approximation (E_2) is always less than the actual value (A_2). These results symmetrically reverse in the case where observations are both taken after their respective transits.

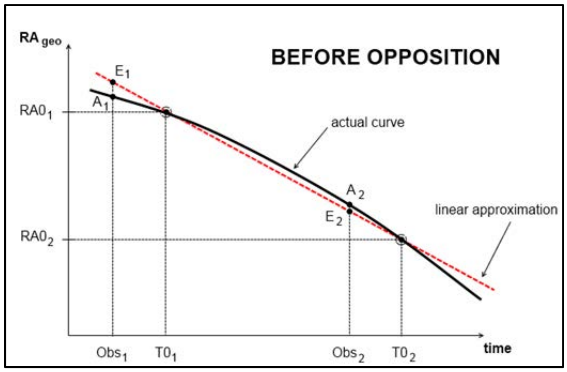

Figure 3. The real apparent retrograde motion in RA of a minor planet before opposition. The instant speed continues to increase until opposition is reached.

Similarly, if the asteroid has already passed opposition, at any given time (Obs_1) prior to that night's transit ($T0_1$) the RA_{geo} value estimated by linear approximation (E_1) is always less than the actual value (A_1). On the contrary, at any given time (Obs_2) prior to the second transit ($T0_2$), the RA_{geo} value estimated by linear approximation (E_2) is always larger than the actual value (A_2). Once again, these results symmetrically reverse in case the observations are both taken after their respective transits.

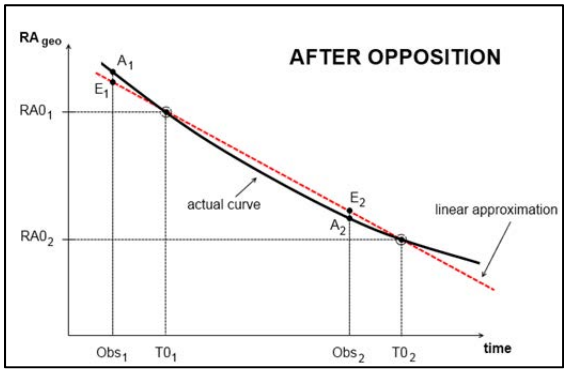

Figure 4. The real apparent retrograde motion in RA of a minor planet after opposition. The instant speed continues to decrease until the loop is ended and direct motion reassumed.

At any given time, the linear rate approximation for the RA_{geo} motion becomes either an over or under estimation for the real RA_{geo} value depending on (a) whether or not the target has yet reached opposition, (b) whether observations are taken at the first or second night of consecutive transits, and (c) whether or not observations are taken from the same side of the

Meridian. According to Equation 1, at any time an over estimation for the RA_{geo} value yields an under estimation for the variable parallactic angle φ, and vice versa. Table 1 summarizes all possible situations. The good thing is that for observations taken from the same side of the Meridian on two consecutive nights – no matter whether the target has or hasn't yet reached opposition – for each night the linear rate approximation gives RA_{geo} values of opposite sign error which consequently make that the derived parallax also yields values of opposite sign error.

	First-night session				Second-night session			
	Before transit		After transit		Before transit		After transit	
	RA_{geo}	φ	RA_{geo}	φ	RA_{geo}	φ	RA_{geo}	φ
Before opposition	+	-	-	+	-	+	+	-
After opposition	-	+	+	-	+	-	-	+

Table 1. The linear rate approximation for the RA_{geo} motion becomes an over estimation (+) or an under estimation (-) for RA_{geo} and φ instant values depending on the moment of observations.

Therefore, observing either before or after opposition, the linear approximation for estimating the unknown RA_{geo} becomes truly appropriate on condition that one averages computations derived from images taken on consecutive nights well separated in time from their corresponding transit times – either both earlier or later, but not mixed up. By averaging the two, computing errors tend to cancel out. This is the pillar supporting our procedure for measuring asteroid parallaxes, requiring just four measurements on two proximate nights (preferably consecutive nights).

On each night, one of the measurements must be done while the target crosses the Meridian, and the other when the target happens to be as far from culmination as possible in order to maximize sensitivity – but on both nights these later measurements should be taken from the same side of the Meridian. We named this simple procedure as the '4-Point Backyard Diurnal Parallax Method'.

From the two measurements taken at transit times, a linear approximation for the target's geocentric motion will be determined. With this information, from each of the two remaining measurements the corresponding variable parallactic angles can be obtained. Typically, one of them will be larger and the other smaller than the "true" parallax. Finally, averaging them gives a minimum-error Diurnal Parallax Maximum Angle for the target in question.

4. The 4-Point Backyard Diurnal Parallax Method

In order to improve accuracy, in practice the required 4 data points will be obtained not from just 4 single observations but instead will be derived from 4 sets of images – two sets around consecutive transits times and two sets far in time from their transits (e.g. soon after the target rises). The "transit sets" are necessarily taken around a particular time – that is, at each corresponding transit – but on the other hand they can be taken along a relatively long time interval without losing data accuracy (the images can be taken over an interval up to 20 minutes). Conversely, the set of images far from transit can be taken at any convenient time, but have necessarily to be obtained within a short span of time (preferably, not longer than 10-15 minutes).

From each night's "transit set" of observations it is possible to determine the target's exact local transit time (*T0*). This crucial parameter for developing the algebraic expression for the geocentric right ascension motion has to be known as precisely as possible. An error of just one second does make difference! This fact imposes a hard restriction on the timing accuracy and therefore the PC clock has to be synchronized to a reliable external timing source prior to attempt any imaging sequence.

Fortunately, *T0* can be easily determined by the observer at the required accuracy. The way to do this is by taking a set of images while the target is around transit time (preferably from a few minutes before transit time to a few of minutes after it). For each image, the corresponding time has to be accurately known and target astrometry has to be precisely measured. Then, the difference between measured target's RA_{topo} and Local Sidereal Time is calculated for each observation. Finally, by using the Intercept function on a spreadsheet the time of transit *T0* and the corresponding *RA0* and *Dec0* can be precisely obtained.

Having determined from observations made on two proximate nights (preferably consecutive) the corresponding parameters *T0*, *RA0* and *Dec0* on each night, then the target's geocentric orbital motion in right ascension and declination can be conveniently represented, in a first approximation, by their respective linear rates derived from those six parameters. In case data from a third consecutive night were also obtained, a better (higher-order) algebraic representation for the target's geocentric motion could be used.

From the remaining two sets of observations – those taken within a relative short time interval as far from culmination as possible but both on the same side of the Meridian (i.e., both either made in the early evening, or both in the pre-dawn) – also corresponding times have to be accurately known and target astrometry has to be precisely measured. Input times and derived astrometric values must both be averaged, so that a single data pair (time versus target's RA_{topo}) results from each set of observations.

Applying Equation 1 to each data pair gives the target's variable diurnal parallax angle for the time of observation. Equations 2 and 3 then give the target's distance (assumed to remain constant over the two nights). Finally, by averaging the target's distance derived from the two data pairs a much more accurate target distance is obtained – as well as the corresponding Diurnal Parallax Maximum Angle.

In our previous study (Alvarez and Buchheim, 2012) we applied the 4-Point Backyard Diurnal Parallax Method on 9 pairs of consecutive nights to find the distance to five asteroids placed from 0.048 au up to 2.56 au. One distance error achieving 6.4%, another 5.8%, and the remaining seven errors showing much lesser percentages proved the validity of the method – at least for parallax angles as low as 3 arcseconds.

5. Pluto Observations

The Pluto dataset consists of images taken in 2012 on 3 pairs of consecutive nights: 8-9 April, 15-16 May, and 25-26-27 July. On each night at least two sets of images were taken: one set when Pluto was relative low in the eastern skies, and a second set while Pluto was transiting the Meridian at an altitude of 78º. The images were obtained using a 12-inch Meade LX-200R working at f/6.9 with an Optec Lepus focal reducer lens and a Quantum Scientific QSI 516wsg non-anti blooming CCD camera, from Observatorio Los Algarrobos, Salto, Uruguay (OLASU), MPC code I38, coordinates: 57.98º W, 31.39º S. The corresponding FOV was 23 x 16 arcminutes.

All images were taken unfiltered. Table 2 is a journal of observations, showing for each night Pluto's local altitude for each set of images, exposure times, CCD temperature, binning, image scale, autoguiding condition and Pluto's visual magnitude. All images were dark and flat-field corrected and then measured using MPO Canopus (Bdw Publishing) version 10.4.0.20.

2012	Altitude (deg)	Expos (s)	CCD temp (ºC)	Binning	Image Scale (arcsec/px)	Guiding	Phase ang (deg)	Visual mag
Apr 08	32 - 78	60	-10	2x2	1.77	No	1.7	14.48
Apr 09	14 - 78	60	-10	2x2	1.77	No	1.7	14.48
May 15	23 - 78	60	-10	2x2	1.77	No	1.2	14.41
May 16	19 - 78	60	-10	1x1	0.89	No	1.2	14.40
Jul 25	34 - 78	60	-15	2x2	1.77	Yes	0.7	14.35
Jul 26	34 - 78	60	-15	2x2	1.77	Yes	0.8	14.36
Jul 27	35 - 78	60	-15	2x2	1.77	Yes	0.8	14.36

Table 2. Observation log for this study.

The first pair of nights (April 8-9, 2012) corresponded when Pluto was changing from direct to retrograde motion – that is, when having almost no motion in right ascension. The second night pair (May 15-16, 2012) corresponded when Pluto was moving retrograde, increasing its RA rate prior to opposition – which took place at June 29, 2012. The final set (July 25-26-27, 2012) corresponded when Pluto was also moving retrograde, but decreasing its RA rate after having past opposition. Figure 5 schematically represents such dates along Pluto's RA motion through middle 2012.

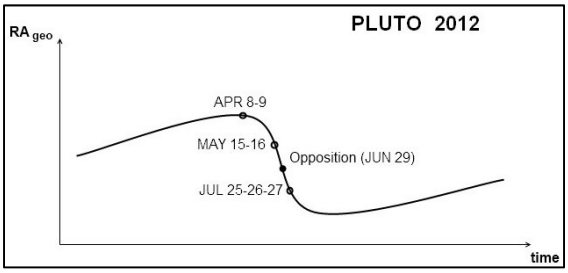

Figure 5. Dates of observing sessions for this study and their correspondence to Pluto's apparent motion in right ascension.

Pluto has a relative big satellite named Charon. It appears almost 2 magnitudes fainter than Pluto, separated about 0.8 arcseconds, and revolving the parent planet each 6.4 days. For this study we selected to work at an image scale (1.77 arcsecond/pixel) large enough to prevent potential errors derived from Charon motion, but still small enough for allow quality astrometry. Only on one night we experimented enlarging resolution (0.89 arcsecond/pixel) but found no practical difference.

6. Differential Astrometry à la Carte

Measuring minute parallax angles requires precision but not accuracy. 'Precision' relates to how many significant decimal places in a given measurement can be confidently stated; 'accuracy' relates to how closely a measurement matches the underlying true value (Buchheim, 2007). Here, our objective is to measure tiny displacements relative to background stars as precisely as possible.

A target's astrometric solution means deriving its celestial coordinates by comparing its position relative to a given set of reference stars – 'differential astrometry'. The modern way to perform differential astrometry is by matching the image in question to a computed stellar chart representing in a plane the corresponding area of the celestial sphere. In theory, measured coordinates of the reference stars appearing on the image should match exactly the computed coordinates on the chart. In practice, this is never the case due to uncertainties in the reference star positions, random errors in the reference star centroids, atmospheric distortions, imaging aberrations, etc.

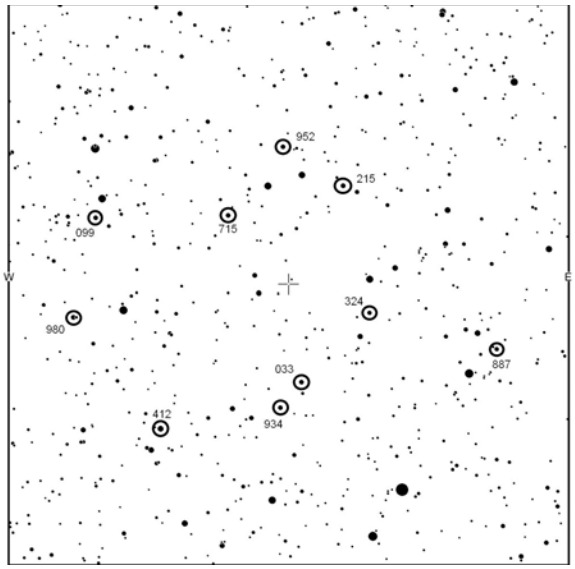

Figure 6. The 15 x 12 arcmin star field around Pluto on May 16th, 2012 (chart centered on coordinates (2000) 18:38:25; -19:14:10). North is down. The reference stars actually used for finding out Pluto's astrometry are labeled according to data in Table 3. Comparatively, the CCD field-of-view used for this study was twice as large (23 x 16 arcmin).

In order to minimize errors, astrometry programs normally use as many reference stars as possible; in other words, all available nearby catalogued stars. This is in general a wise practice – but not for our specific purpose of measuring Pluto's parallax. At our required subarcsecond precision astrometry, performed on images necessarily taken at very different sky altitudes, atmospheric refraction inevitably distorts the relative position of different color stars as air mass varies.

Chart star	Name (3UCAC)	RA (h:m:s)	DEC (deg:m:s)	Color index (B-V)	Visual magnitude
412	142-337412	18:38:10.55	-19:10:17.4	1.10	11.76
215	142-338215	18:38:31.21	-19:16:48.0	0.67	12.47
033	142-338033	18:38:26.49	-19:11:32.5	0.63	12.48
952	142-337952	18:38:24.42	-19:17:50.9	1.09	12.50
980	142-336980	18:38:00.63	-19:13:16.8	0.64	12.51
934	142-337934	18:38:24.09	-19:10:51.7	0.62	12.53
715	142-337715	18:38:18.17	-19:16:00.1	0.99	12.59
324	142-338324	18:38:34.19	-19:13:24.2	1.09	12.62
099	142-337099	18:38:03.16	-19:15:56.0	0.73	12.63
887	142-338887	18:38:48.63	-19:12:25.4	0.76	12.74

Table 3. The exclusive reference stars set used for deriving Pluto's astrometry on all images taken on May 15 and 16, 2012.

Therefore, we avoid this by selecting a particular set of reference stars – those that happen to be about the same color index as Pluto (B-V = 0.8) and placed nearby around it, preferentially at about the same angular distance from Pluto. The same stars are used on both consecutive nights, to avoid any errors caused by using separate arrays of reference stars. Figure 6 shows which the chosen stars were for the nights of May 15 and 16, and Table 3 summarizes corresponding data.

In effect, Pluto's astrometry data derived from the selected set of 10 reference stars did differ from data automatically obtained from the whole set of 75 available nearby stars. Table 4 compares the values for observations taken on May 16, 2012. The first 10 images were taken at a sky altitude of 19º, while the other 10 images were taken about 5 hours later, around Pluto's culmination at an altitude of 78º. For those taken earlier at low altitude (that is, from those where the parallactic angle was going to be later derived), both Pluto's RA and DEC yield relative large and consistent differences depending on the reference stars used (shown in the last two columns).

UT time	RA from selected ref	DEC from selected ref	RA from all nearby stars	DEC from all nearby stars	Difference in RA sec	Difference in DEC sec
1:33:22	18:38:22,753	-19:14:11,95	18:38:22,738	-19:14:12,02	+0.015	-0.07
1:34:28	18:38:22,736	-19:14:11,84	18:38:22,736	-19:14:11,85	0.000	-0.01
1:35:33	18:38:22,786	-19:14:11,90	18:38:22,744	-19:14:12,01	+0.042	-0.11
1:40:15	18:38:22,718	-19:14:12,04	18:38:22,714	-19:14:12,14	+0.004	-0.10
1:41:20	18:38:22,731	-19:14:11,96	18:38:22,710	-19:14:12,11	+0.021	-0.14
1:42:26	18:38:22,730	-19:14:11,79	18:38:22,718	-19:14:11,87	+0.012	-0.08
1:43:31	18:38:22,730	-19:14:11,83	18:38:22,703	-19:14:11,98	+0.027	-0.15
1:44:37	18:38:22,716	-19:14:12,03	18:38:22,695	-19:14:12,19	+0.021	-0.16
1:45:42	18:38:22,714	-19:14:12,05	18:38:22,702	-19:14:12,16	+0.012	-0.11
1:46:47	18:38:22,726	-19:14:12,04	18:38:22,708	-19:14:12,03	+0.018	+0.01
6:47:26	18:38:21,810	19:14:13,09	18:38:21,814	19:14:13,12	-0.004	-0.03
6:48:31	18:38:21,810	19:14:13,11	18:38:21,810	19:14:13,13	0.000	-0.02
6:49:36	18:38:21,814	19:14:13,07	18:38:21,811	19:14:13,11	+0.003	-0.04
6:50:42	18:38:21,817	19:14:13,05	18:38:21,813	19:14:13,08	+0.004	-0.03
6:51:47	18:38:21,807	19:14:13,09	18:38:21,807	19:14:13,12	0.000	-0.03
6:52:52	18:38:21,784	19:14:13,08	18:38:21,803	19:14:13,13	-0.019	-0.05
6:53:58	18:38:21,792	19:14:13,13	18:38:21,798	19:14:13,11	-0.006	+0.02
6:55:03	18:38:21,798	19:14:13,13	18:38:21,799	19:14:13,13	-0.001	0.00
6:56:09	18:38:21,790	19:14:13,18	18:38:21,790	19:14:13,18	0.000	0.00
6:57:14	18:38:21,785	19:14:13,04	18:38:21,782	19:14:13,04	+0.003	0.00

Table 4. Comparison of Pluto's astrometry for the 20 images taken on May 16, 2012, derived from the exclusive 10 reference stars set (second and third column) to corresponding astrometry automatically derived from nearby 75 reference stars set (fourth and fifth columns). Relative differences (in seconds) are showed in the last two columns.

The same procedure was performed for each one of the April and July imaging sessions. This tedious homework was the indispensable toll allowing us to safely cross the labyrinth towards the good subarcsecond data exit. Astrometric measurements derived from 'standard' (automatically performed) astrometry on the same star field imaged at quite different sky altitudes was simply not precise enough for the hard requirements imposed at the subarcsecond level. As a matter of fact, none of our previous successful asteroid parallax measurements required differential astrometry à la carte; however, dealing with Pluto showed us there was no other way but to roll up our sleeves and just do it.

7. Data Assessment and Final Analysis

Once Pluto's differential astrometry was derived from a carefully selected set of reference stars, the next step was to determine corresponding *T0* and

RA0 from each set of 10 images taken while Pluto was very close to the Meridian. From each pair of consecutive nights, a linear approximation for the geocentric right ascension was immediately derived. Knowing the linear RA rate it was possible to determine the variable diurnal parallax angle for each image.

The next task was to assess the quality of achieved data around each transit time. This assessment was performed by finding the average variable parallactic angle and its standard deviation for those sets embracing culmination (in a perfect world, both the average variable parallactic angle and the standard deviation would have been zero). Then, data differing from the average by more than one standard deviation were rejected, so that a new *T0* and *RA0* were recomputed. To illustrate this move, Table 5 presents in particular the ten measurements obtained around Pluto's culmination on July 27, 2012, and identifies which ones were rejected due to notorious differences from the average value.

UT Time	RA measured	LST	RA - LST	φ derived	φ average	Rejected
01:54:43	18,52162278	18,45597311	-0,0656	0,116	**-0,002**	X
01:55:46	18,52162028	18,47352102	-0,0481	0,045		
01:56:49	18,52161583	18,49106894	-0,0305	-0,125	**std dev**	X
01:57:52	18,52161444	18,50861685	-0,0130	-0,139	**0,093**	X
01:58:55	18,52161778	18,52616476	0,0045	0,087		
01:59:58	18,52161333	18,54371268	0,0221	-0,082	**φ avg + std dev**	
02:01:01	18,52161639	18,56126059	0,0396	0,130	**0,091**	X
02:02:04	18,52161167	18,57880850	0,0572	-0,054		
02:03:06	18,52161222	18,59607788	0,0745	0,030	**φ avg - std dev**	
02:04:09	18,52161000	18,61362579	0,0920	-0,027	**-0,095**	

Table 5. Data corresponding to the transit set of July 27, 2012 (July, Observing session #3).

Rejecting discordant data had no influence on the corresponding *T0* but did modify – although slightly – the resulting *RA0*. Figure 7 shows this effect for the data presented in Table 5. At top, the original data from the 10 observations gave *RA0* = 18.52161635 h, while after rejecting the first, third, fourth and seventh observations, the obtained value at bottom was *RA0* = 18.52161669 h (a minuscule difference of just 0.00000034 h). However, these sifting certainly improved the final quality of our results. This exemplifies how challenging the realm where subarcseconds rule actually is. No such data iteration had been required in our previous study, as measurement errors were comparatively smaller here.

Now it was time to compute the variable parallactic angle for the sets of images taken far away from culmination. Figure 8 presents all variable parallactic angles measured for each night. The plot for July 2012, Observing session #2 (July 26, 2012) appears twice because it was part of two different pairs (July 25-26 and July 26-27) so that the same input processed by means of different RA_{geo} linear approximations certainly gave different results.

Similarly as was done for the transit sets, for each low-altitude set the average variable parallactic angles and the standard deviations were determined. Once again, data differing from the average by more than one standard deviation were rejected. The remaining data were used to determine a single parallactic angle, which corresponded to the average time of the accepted low-altitude data. By means of Equations 2 and 3, Pluto's distance and the corresponding Diurnal Parallax Maximum Angle were found for each observing session.

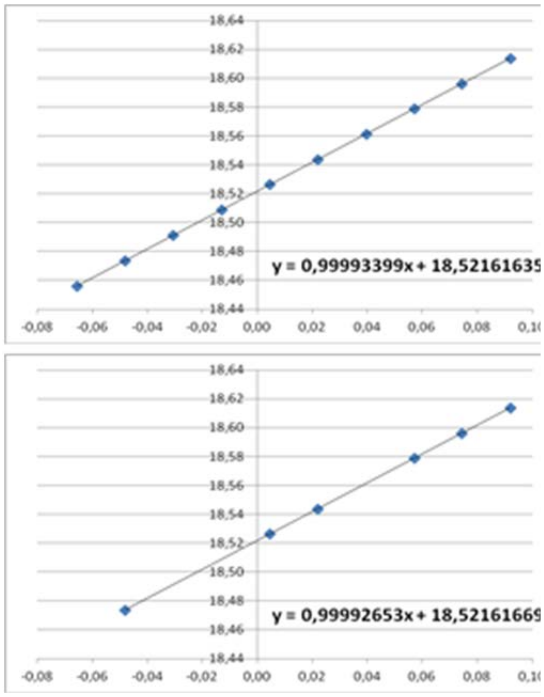

Figure 7. The graph at top shows the original ten measurements obtained around transit of July 27, 2012. The corresponding exact intercept value is *RA0* = 18.52161635 h. Once the 'bad' data were eliminated (from the left, the first, third, fourth and seventh points) the new intercept value changed to *RA0* = 18.52161669 h, as seen in the bottom graph.

Session	Date	Actual distance (au)	Actual φ_{max} (arcsec)	Found distance (au)	Distance error (%)	Found φ_{max} (arcsec)	φ_{max} error (%)
1	2012/04/08	32.034	0.234	77.090	140.7	0.097	-58.5
2	2012/04/09	32.018	0.234	17.740	-44.6	0.423	80.8
1+2	**2012/04/08-09**	**32.026**	**0.234**	**47.415**	**48.1**	**0.158**	**-32.5**
3	2012/05/15	31.502	0.238	35.131	11.5	0.213	-10.5
4	2012/05/16	31.491	0.238	16.191	-48.6	0.463	94.5
3+4	**2012/05/15-16**	**31.497**	**0.238**	**25.661**	**-18.5**	**0.292**	**22.7**
5	2012/07/25	31.354	0.239	18.737	-40.2	0.400	67.4
6	2012/07/26	31.362	0.239	38.772	23.6	0.193	-19.2
5+6	**2012/07/25-26**	**31.358**	**0.239**	**28.755**	**-8.3**	**0.261**	**9.2**
6	2012/07/26	31.362	0.239	21.445	-31.6	0.350	46.4
7	2012/07/27	31.370	0.239	45.592	45.3	0.164	-31.4
6+7	**2012/07/26-27**	**31.366**	**0.239**	**33.519**	**6.9**	**0.224**	**-6.3**
5 (q)	2012/07/25	31.354	0.239	24.561 (q)	-21.7	0.305 (q)	27.6
6 (q)	2012/07/26	31.362	0.239	29.439 (q)	-6.1	0.255 (q)	6.7
7 (q)	2012/07/27	31.370	0.239	33.055 (q)	5.4	0.227 (q)	-5.0

Table 6. Results from each one of observing sessions. Except for the last three rows, corresponding *RAgeo* motion was replaced by a linear representation; for the last three rows it was used a quadratic representation.

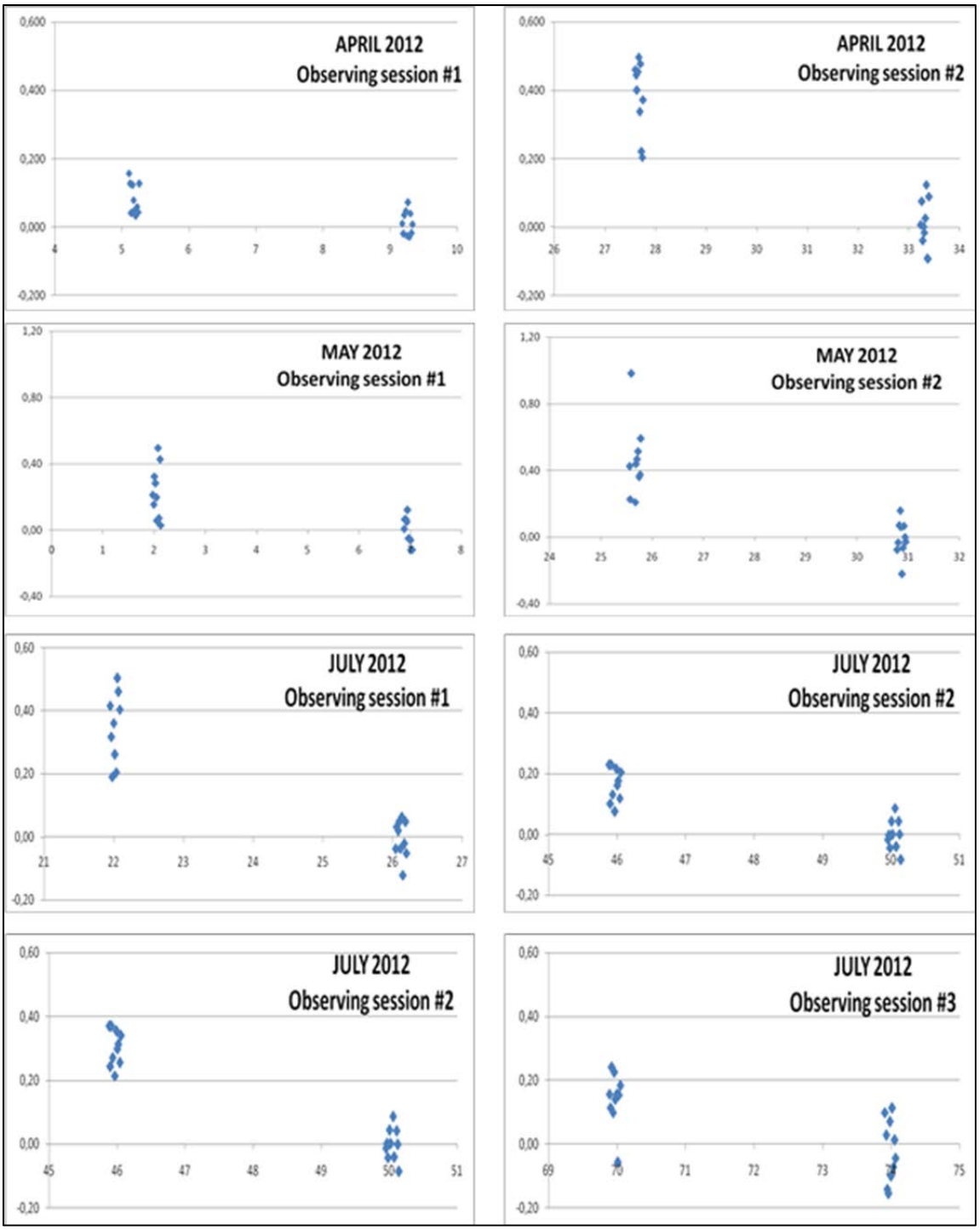

Figure 8. Variable diurnal parallax angles (expressed in arcseconds) obtained along each observing night for this study, by means of using a linear approximation for the geocentric RA motion. Horizontal axes correspond to respective elapsed times (in hours). July 26, 2012 data (July 2012, observing session #2) appears twice, as it was used as the second-night data for the pair July 25-26, and as the first-night data for the pair July 26-27. Outlying values (that is, data lying outside the 'normal' range defined as the average values plus or less corresponding standard deviations) were later on rejected. According to Table 1, April and May sessions (prior to opposition) gave smaller φ values for each first-night session (when *RAgeo* was overestimated) compared to those for corresponding second-night session (when *RAgeo* was underestimated), while the opposite happened for July sessions (past opposition).

Table 6 presents the final results (Pluto's distance and Diurnal Parallax Maximum Angle). As already discussed, averaging results from each pair of observing sessions yielded much better values, as errors from the two nights have opposite signs and tend to cancel out.

All but the last three rows correspond to results obtained from a linear approximation for the RA_{geo} motion. Distance error for the first pair of sessions was pretty large (48.1%), somehow confirming that the 4-Point Backyard Diurnal Parallax Method is not suitable near the "stationary point", where the target is reversing its motion (either from direct to retrograde motion or vice versa). On the other hand, distance errors for the remaining pairs – those corresponding to when Pluto was frankly within retrograde motion – were quite good (-18.5%, -8.3% and 6.9%).

All these outcomes firmly confirm the usefulness of the 4-Point Backyard Diurnal Parallax Method for determining the distance to any asteroid near opposition. The method needs a total observation time of only 40 minutes on two consecutive nights, with modest amateur equipment. However, dealing with parallaxes at the subarcsecond level does require much more care at the data processing stages as compared to the "usual" handling for main-belt asteroids. In particular, it is indispensable that (a) astrometry should be done by using only a selected appropriate set of reference stars, and (b) input data must be scrutinized in order to get rid of those slightly discordant values that otherwise would degrade results.

Finally, we tested a slightly different approach for handling the target's proper motion. Instead of using a linear representation for Pluto's geocentric right ascension, derived from transit data from two consecutive nights, we took advantage of having three consecutive nights observed in July. From the three transit observations we were able to obtain a more accurate quadratic representation of Pluto's RA_{geo} vs. time. The analytical equations for the linear and quadratic solutions are showed in Figure 9.

The numerical difference between them appears only at the sixth decimal place. For instance, the corresponding RA_{geo} values for t = 45 hours are RA_{geo}(linear) = 18.5234566 h and RA_{geo}(quadratic) = 18.52345547 h. Once again, despite this minuscule absolute difference, exactly the same data input yields noticeably different results, as showed in Figure 10. For each night, the relative variable parallactic angle distribution remains the same, but due to the more accurate RA_{geo} representation the data bundle clearly moves vertically at right in the 'right' direction – downwards for Observing sessions #1 and 2b (i.e., those first-night sessions for which a RA_{geo} linear rate yielded overestimated parallax angles), and upwards for Observing sessions #2a and 3 (i.e., those second-night sessions for which a RA_{geo} linear rate yielded underestimated parallax angles).

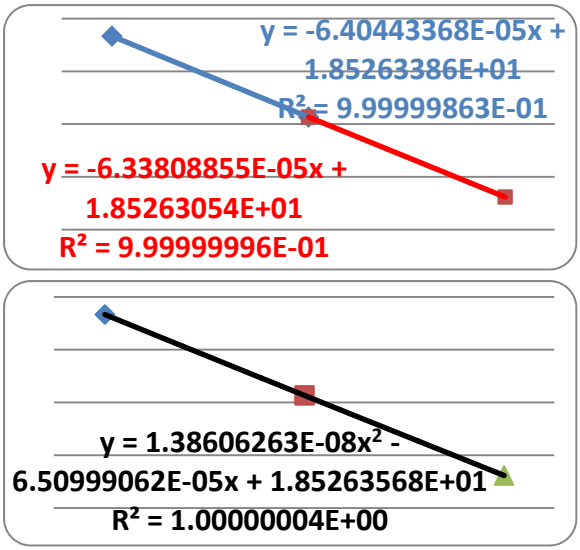

Figure 9. The 3 data points appearing in both graphs are exactly the same – they are Pluto's *T0* and *RA0* for July 25, 26 and 27, 2012. At top, the two different linear segments joining such data points and corresponding analytical expressions; at bottom, the single second-order curve joining such data points and corresponding analytical expression. Due to the fact that we are dealing with minuscule differences, neither the graph at the top appears to show two different tilted lines – as it's actually the case – nor the graph at the bottom appears to show a curve (with a positive concavity) – as it's also the actual case (and at the same time a much accurate representation of Pluto's *RAgeo* (*t*) while in retrograde motion after opposition).

The last three rows of Table 6 correspond to results obtained by means of a quadratic representation for the geocentric right ascension. In these cases, errors for Pluto's distance derived from direct observation – not from averaging any pair of underestimated and overestimated values – were quite satisfactory (respectively, -21.7%, -6.1% and 5.4%) at the price of requiring one more transit data than the Spartan 4-Point Backyard method.

8. Further Work

The distance to nearby stars can be accurately determined by measuring their parallax angle while the Earth orbits around the Sun. The geometry of this situation is exactly the same as drawn in Figure 1, except that now the circumference represents the orbit of the Earth. As the Earth orbits around the Sun, any observer on its surface sees the star's parallactic angle φ constantly varying, from a maximum value occurring whenever the Earth is at right angle to the

plane perpendicular to the Ecliptic which also contains both the Sun and the star (some 3 months prior or after star due opposition) to a null value whenever the Earth happens to also be placed on such plane (star opposition).

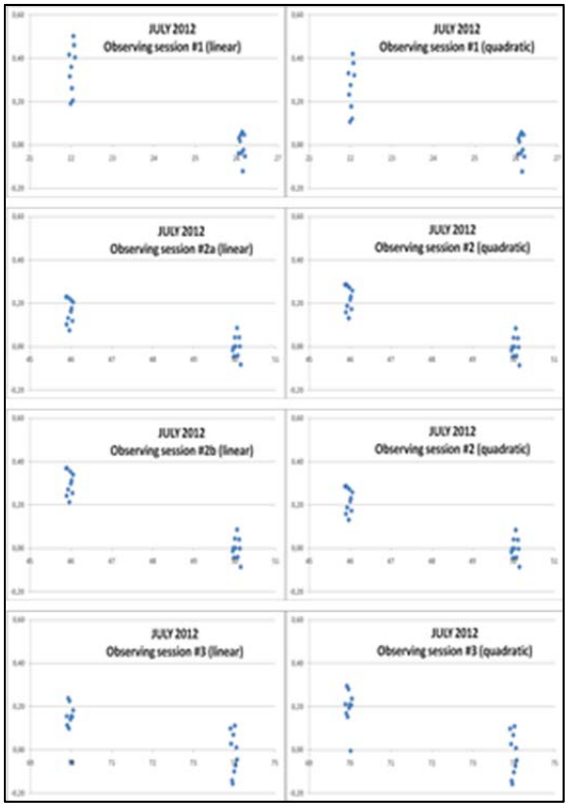

Figure 10. Comparison of the same input data but having been processed via different representations for Pluto's RA motion (at left, by linear rates; at right, by quadratic rates). Due to the more accurate quadratic rate, bundle data from first-night sessions (first and third rows) appear at right moved down, while bundle data from second-night sessions (second and fourth rows) appear at right moved up – in accordance with the discussed φ errors introduced by a linear representation for Pluto's RA_{geo} retrograde motion past opposition for observations prior to culmination (see Table 1).

If the beginning of the time parameter is strategically selected to coincide with the moment of the star opposition, then our reasoning for the diurnal parallax effect is completely equivalent for the star parallax case – and hence, the related equations can be accordingly translated. The "exact time of the asteroid culmination" now becomes the "exact time of the star opposition", and the "geocentric motion of the asteroid" now becomes the "proper motion of the star". Otherwise the formulation will be identical.

Therefore, the 4-Point Backyard Diurnal Parallax Method would work basically the same for the distance determination of a nearby star – except this time to collect the four data points will span 15 months instead of just 30 hours.

Considering that the parallax angle of nearby stars is about the same as Pluto's (Sirius' annual parallax is actually 60% larger than Pluto's diurnal parallax), the parallactic determination of their distance seems to be a feasible task and therefore our next logical challenge to face.

9. Conclusions

Although this project does not deliver any new science results, it is a wonderful educational experience and it provides a convenient "dry run" for attempts to measure stellar parallax. Both stellar (annual) parallax and Pluto (diurnal) parallax demand astrometric precision of better than 0.1 arcsecond; but the "Pluto" project can be done in a few nights, whereas the stellar annual parallax requires observations spanning about 15 months. The "Pluto" project highlights careful procedures that are needed for precision parallax determinations: selection of a consistent set of astrometric reference stars, and having a method of dealing with the target's proper motion (orbital motion in the case of Pluto). For both Pluto and nearby-star parallax, the target's proper motion may be of the same order of size as the parallax, so both effects must be dealt with in any parallax project.

The good-accuracy results achieved here were probably helped by the southern-hemisphere location of OLASU, where the observations were made. Pluto's southerly declination placed it high in the sky at transit, when viewed from Uruguay.

There is a curious oddity in these results, in that the 4-Point Backyard Diurnal Parallax Method works best when the target is near opposition. This is in contrast to the early historic asteroid parallax measurements that were used to determine the scale of the Solar System. The early investigators selected nights where the asteroid was "stationary" as their way of minimizing the effect of relative orbital motion between Earth and asteroid. The "4-point" method, on the other hand, works best near opposition (when the Earth-target relative rate is maximum) because it uses a model of constant-speed relative motion. With the "4-point" method, the important consideration is that the target's relative orbital motion be non-accelerating, which is best achieved near opposition. This incentive for doing the project near the time of the target's opposition probably makes it more convenient for student projects. It certainly makes for more flexible scheduling of the observing nights, since any convenient pair of consecutive nights within about a month of opposition can be used.

10. References

Alvarez, E.M., Buchheim, R.K. (2012). Diurnal Parallax Determinations of Asteroid Distances Using Only Backyard Observations from a Single Station. i*n Proceedings for 31st Annual Symposium on Telescope Science* (Warner *et al.*, eds.) pp.45-58. Society for Astronomical Sciences, Rancho Cucamonga, CA.

Berry, Richard (2011). The Proper Motion and Parallax of Barnard's Star: Errors and Precision in Small-Telescope Astrometry. *in Proceedings for 30th Annual Symposium on Telescope Science* (Warner *et al.*, eds.) pp.79-86. Society for Astronomical Sciences, Rancho Cucamonga, CA.

Buchheim, Robert K. (2007). *The Sky is Your Laboratory: Advanced Astronomy Projects for Amateurs.* Springer-Praxis Publishing Ltd., New York.